

Crystallinity and chain orientation of injection-molded poly(butylene terephthalate) depending on the depth profile at the surface

Masanori Haga¹, Takahiko Nakaoki^{1,*}, Hideaki Ishihara¹, Katsuhisa Yamashita²
and Kenichi Funaki²

¹Department of Materials Chemistry, Ryukoku University, Seta, Otsu, Shiga 520-2194, Japan;

²Toyobo Co., Ltd., 2-1-1 Katata, Otsu, Shiga 520-0292, Japan.

ABSTRACT

The proposed study aims to investigate the relationship between the crystallinity and chain orientation of injection-molded poly(butylene terephthalate) (PBT) as a function of depth profile using thermal analysis, X-ray diffraction, and polarized infrared (IR) spectroscopy. The crystallinity determined by differential scanning calorimetry (DSC) decreased from the skin to core layers, whereas that determined by X-ray diffraction increased from the skin to core layers. The difference in crystallinity determined by DSC and X-ray diffraction is due to the formation of a mesophase, which is formed in the skin layer due to the presence of the shear stress. The chain orientation was observed by polarized attenuated total reflection (ATR)-IR spectroscopy. At the gate of PBT plate, the dichroic ratio at 874 cm⁻¹ was about 0.8 and 0.5 near the skin layer, whereas it reached around 1.0 and 0.75 at the core layer for PBT formed at injection molding rates of 40 and 80 mm/s, respectively, corresponding to the increased chain orientation in the skin layer. This indicated that more mesophase was formed due to the shear stress at the skin layer.

KEYWORDS: poly(butylene terephthalate), injection mold, skin-core, crystallinity, molecular orientation.

INTRODUCTION

Poly(butylene terephthalate) (PBT) is a representative engineering plastic with a fast crystallization rate. Injection molding is widely used for processing polymers. It was reported that injection-molded PBT adopts a skin-core structure [1-9]. From the viewpoint of practical use, a fast crystallization rate is an advantage as it shortens the injection molding cycle. However, a large temperature gradient and shear stress between the polymer surface and mold wall induce a skin-core structure. Generally, a comparatively fast cooling rate and high shear stress in the skin layer lead to a lower crystallinity and higher orientation than that in the core layer. It was reported that the thickness of the skin layer of injection-molded PBT ranges from 20 to 200 μm depending on the melt and mold temperature, and no spherulites were present in the skin layer, while many were observed in the core layer [1]. Rhoades *et al.* identified crystallization in the skin and core layers by fast scanning chip calorimetry and microfocus X-ray diffraction [7]. The crystallinity of the skin layer was lower than that of the core layer.

Regarding the crystal structure of PBT, both α- and β-forms exist [10-21]. The α-form is stable with a gauche-trans-gauche (gtg) conformation at the methylene sequence, whereas the β-form is induced during stretching and adopts an extended structure with a trans-trans-trans (ttt) conformation at the methylene sequence. The β-form is a

*Corresponding author: nakaoki@rins.ryukoku.ac.jp

quasi-stable state, which transforms to the α -form when there is no stretching stress. It is worth noting that a mesophase exists for PBT [22]. This is reportedly induced by stretching, but it contains no regular unit cells such as those in crystals. The PBT main chain is rigid, providing one-dimensional regularity along the chain axis, corresponding to a liquid crystal-like structure. When a PBT plate is formed by injection molding, the shear stress between the plate and mold wall is an important factor in crystallization. Thus, this crystallization has been investigated under shear stress [23, 24]. It was reported that crystallization increases with the shear rate.

The mesophase plays an important role in determining the physical properties, but only a few investigations have been conducted on the mesophase of injection molded PBT. In this study, the relation between the crystallinity and chain orientation was investigated as a function of depth profile for PBT formed at injection molding rates of 40 and 80 mm/s.

MATERIALS AND METHODS

Two types of injection-molded PBT plates formed at injection molding rates of 40 and 80 mm/s were supplied by Toyobo Co., Ltd. These are abbreviated as PBT₄₀ and PBT₈₀, respectively. The plate size was 10 cm × 10 cm × 2 mm. No additive was used. The PBT plate was sliced from the surface with a Leica Microsystems SM2500S instrument and each slice was 25 μ m thick. For the measurements, squares of 1 × 1 cm at the gate, center, and end were used, as shown in Figure 1.

Thermal analysis

Differential scanning calorimetry (DSC) was performed with a Rigaku DSC 8231 instrument. Samples were heated from room temperature to 300 °C at a heating rate of 10 °C/min. The temperature and enthalpy were calibrated with indium.

X-ray diffraction

X-ray diffraction was performed using SPring-8 (BL03XU, Issue numbers: 2013A7214, 2013B7262). The beam was focused on the cross section of the PBT plate. The beam diameter was 8 μ m, and the measurement was performed every 10 μ m from the surface.

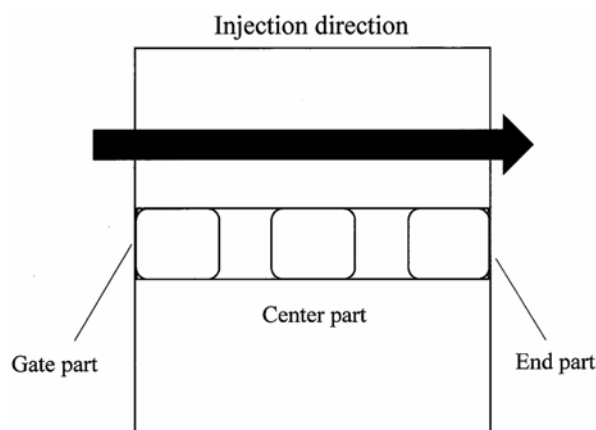


Figure 1. Schematic model of injection-molded PBT plate (10 cm × 10 cm × 2 mm). The plate was sliced from the gate to the end part.

Infrared spectra

Fourier transform infrared spectroscopy (FT-IR) was performed with a JASCO FT-IR 660Plus spectrometer. The resolution was 2 cm⁻¹ with 16 accumulations. For attenuated total reflection (ATR), an ATR PRO 450-S attachment with a diamond prism was used. To obtain an accurate dichroic ratio, the polarized spectra were measured by rotating the sample, as shown in Figure 2. The parallel and perpendicular components were defined as the spectra parallel and perpendicular to the chain flux from the gate to the end of the mold plate. The ATR-IR absorption strongly depends on the contact between the sample and prism. Thus, the peak at 2897 cm⁻¹, which is assignable to the C–H stretching mode irrespective of the crystallinity, was used as an internal standard.

RESULTS AND DISCUSSION

Comparison of crystallinity estimated by DSC and X-ray diffraction

Figure 3 (A) and (B) shows DSC charts of samples sliced from the center part as a function of the depth profile at the plate surface for PBT₄₀ and PBT₈₀, respectively. The endothermic peak due to crystal melting was almost constant at around 224 °C, irrespective of the depth profile, indicating the formation of similar lamellar thicknesses. However, the melting enthalpy depended on the depth profile. The crystallinity (X_c) was estimated from the observed melting enthalpy (ΔH_f) as follows:

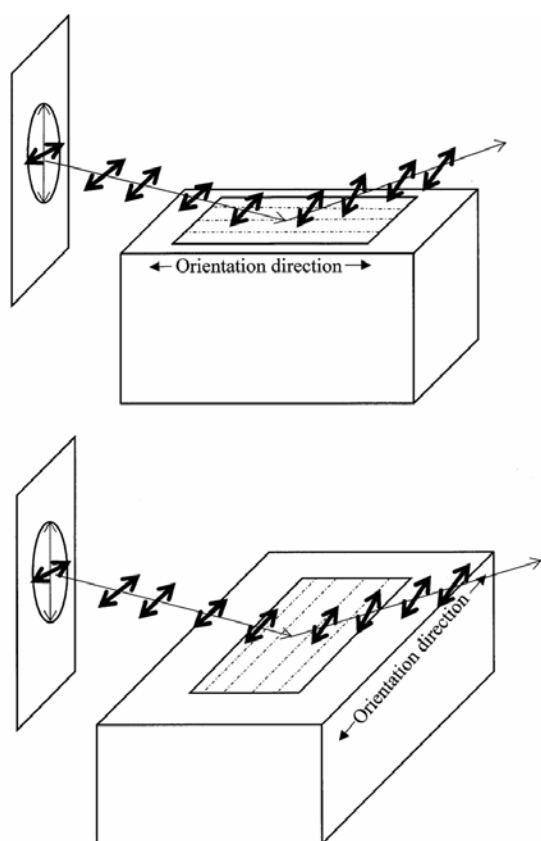


Figure 2. Relationship between the polarization direction of the incident IR beam and the chain orientation.

$$X_c(\text{DSC}) = \frac{\Delta H_f}{\Delta H^\circ} \times 100, \quad (1)$$

where ΔH° denotes the melting enthalpy of a pure crystal for which a value of 145 J/K was adopted [25]. The crystallinity was plotted as a function of the depth profile at the surface, as shown by closed circles in Figure 4. The crystallinity of the skin layer was about 33% and 42% for PBT₄₀ and PBT₈₀, respectively. These values are comparable with the result by Rhoades *et al.*, who reported that the crystallinity of the skin layer was 35% and 42% at the gate and end parts, respectively [7]. The crystallinity of the core layer gradually decreased for both PBTs. Generally, when the injection mold plate was cooled from the melt, the temperature decreased from the plate surface. Thus, the temperature of the core layer decreased more slowly than that of the skin layer. Due to this time lag, the crystallinity of the core layer tends to be higher. However, the experimental result showed

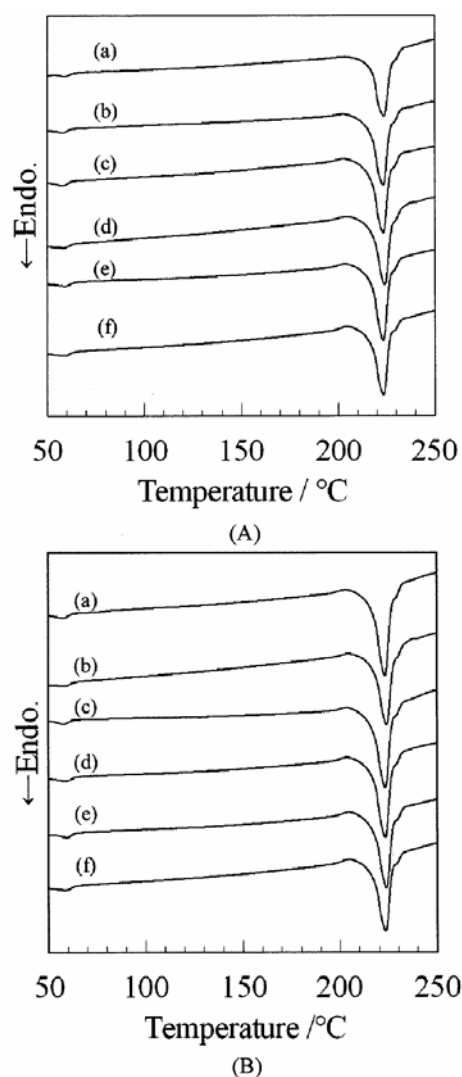


Figure 3. DSC charts of PBT₄₀ (A) and PBT₈₀ (B) depending on the depth profile. (a) 0-25, (b) 75-100, (c) 175-200, (d) 275-300, (e) 375-400, and (f) 475-500 μm .

the opposite trend; i.e., the crystallinity of the skin layer was higher. Considering the dependence on molding rate, the crystallinity of PBT₈₀ was higher than that of PBT₄₀ irrespective of the depth profile. These results can be explained by the formation of a mesophase induced by the shear stress between the PBT and mold plate. The mesophase is not completely amorphous but has a structure with a small endothermic enthalpy of formation. Thus, DSC reflects the endotherm for not only the crystal but also the mesophase. Therefore, the crystallinity of both the crystal and mesophase was estimated by DSC. Rhoades *et al.*

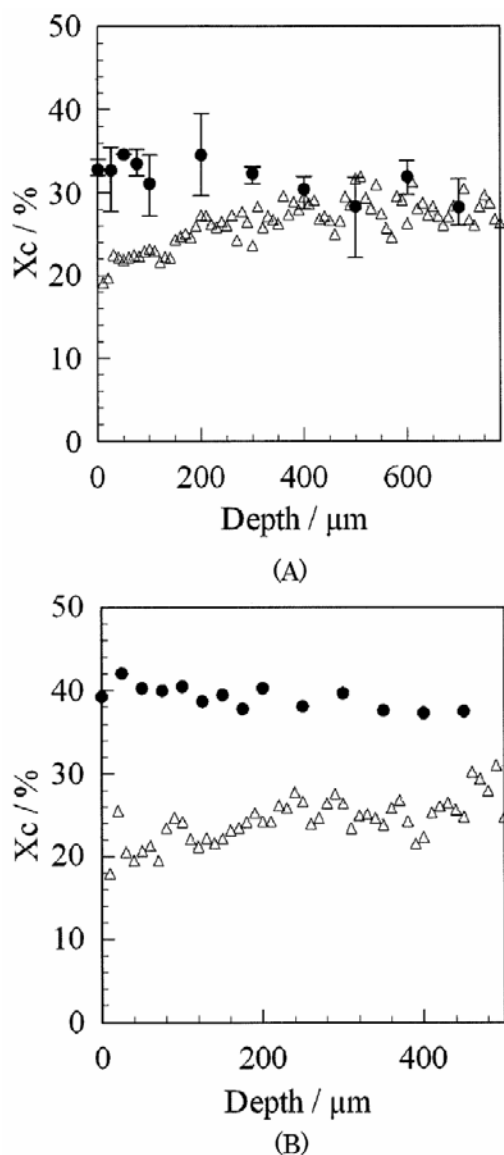


Figure 4. Crystallinity of PBT₄₀ (A) and PBT₈₀ (B) determined by DSC (●) and X-ray diffraction (Δ).

showed that the crystallinity was low and high for the skin and core layers, respectively [7]. This might be explained by the heating rate for DSC; we adopted a heating rate of 10 °C/min, whereas they used a much higher heating rate of 2000 °C/min. This would not reflect the melting enthalpy of the mesophase, because the melting peak observed by Rhoades *et al.* was sharper than that obtained in this work.

X-ray diffraction is another method for determining the crystallinity. Since only regular structures with

a repeating morphology are reflected in X-ray diffraction patterns, the mesophase with no regular structure is regarded as a non-crystalline state. Figure 5 shows X-ray diffraction patterns as a function of the depth profile observed with SPring8. The diffraction peaks for the crystal at 16.1°, 17.4°, 20.8°, 23.5°, and 25.4° were weak for the skin layer; however, these increased in intensity for the core layer. This indicates that the crystallinity of the skin layer was lower than that of the core layer. This is a well-accepted trend. The crystallinity determined by X-ray diffraction was estimated as follows:

$$X_c(\text{X-ray}) = \frac{S_c}{S_c + S_a} \quad (2)$$

where S_c and S_a are the peak areas for the crystalline and non-crystalline areas, respectively. The crystallinity estimated from Eq. (2) was plotted against the depth profile at the skin layer, as shown by open triangles in Figure 4. The crystallinity was 20% in the skin layer and gradually increased for the core layer for both PBTs. The difference in crystallinity determined by DSC and X-ray diffraction for the skin layer was larger than that for the core layer. This is because the formation of a mesophase due to shear stress in the skin layer increased the crystallinity determined by DSC. The fraction of mesophase (X_m) estimated by subtracting the crystallinity obtained by X-ray diffraction from that obtained by DSC is plotted in Figure 6. The fraction of mesophase for PBT₈₀ reached 21% in the skin layer and decreased to 15% in the core layer, whereas that for PBT₄₀ was 14% and 1% in the skin and core layers, respectively. Since the mesophase is induced by orientation processes, such as stretching and shearing, the high fraction of mesophase in the skin layer is due to the shear stress between the PBT plate surface and the mold wall. For the core layer, the shear is comparatively small, and hence the fraction of mesophase is low. The higher fraction of mesophase for PBT₈₀ can be explained by higher chain orientation due to a high injection molding rate. Thus, the chain orientation was investigated as a function of the depth profile using polarized IR, as described in the following section.

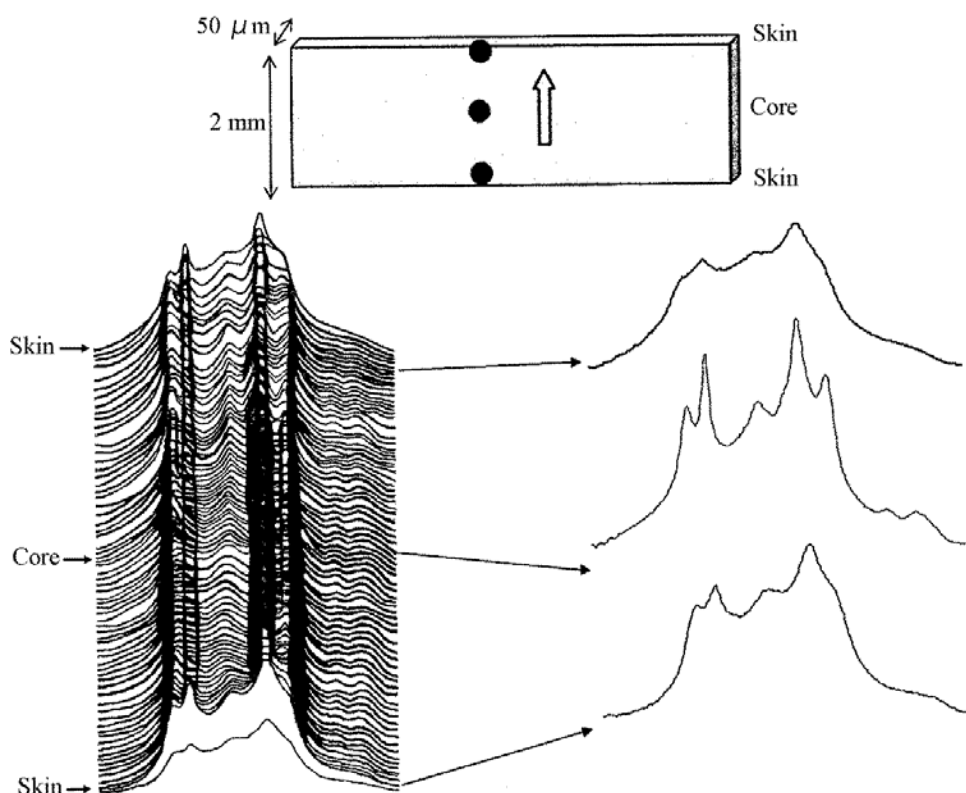


Figure 5. X-ray diffraction patterns as a function of depth profile. The plate thickness was 2 mm, and observations were made every 10 μm from the skin layer.

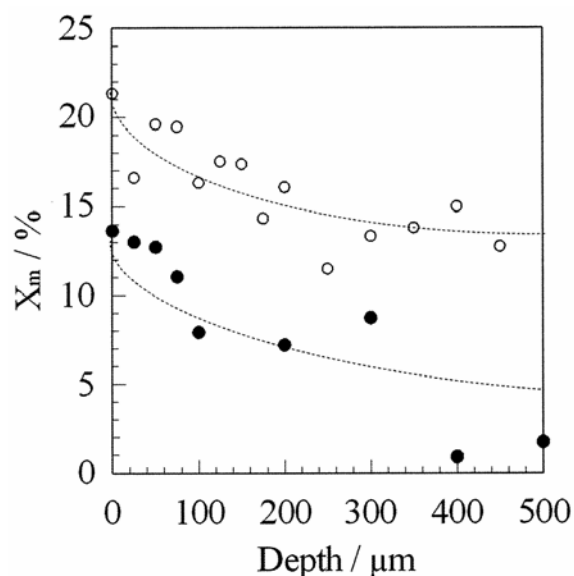


Figure 6. Fraction of mesophase estimated from the difference in crystallinity between DSC and X-ray diffraction; \bullet and \circ correspond to PBT₄₀ and PBT₈₀, respectively.

Chain orientation at the gate of the mold plate

The chain flux is large at the gate of the mold plate. To determine the chain orientation, polarized ATR-IR spectroscopy was performed at the gate part. Figure 7 shows the spectra for the skin and core layers for PBT₄₀ and PBT₈₀. The vibrational peaks at 725 and 874 cm^{-1} are crystalline-sensitive bands, and both peaks are assignable to the C–H out-of-plane mode of the phenylene group of PBT. The stable crystal structure of PBT is the α -form, which has a triclinic unit cell with a *gtg* conformation at the methylene sequences. Thus, the phenylene group in the main chain tilts from the *c*-axis in the unit cell. Therefore, the perpendicular component is larger for the C–H out-of-plane mode of the phenylene group. The perpendicular components at 725 and 874 cm^{-1} were more intense than the parallel ones in the spectra of the skin layers for both PBT₄₀ and PBT₈₀. In the core layer spectra, the intensity ratio of the parallel and perpendicular components is

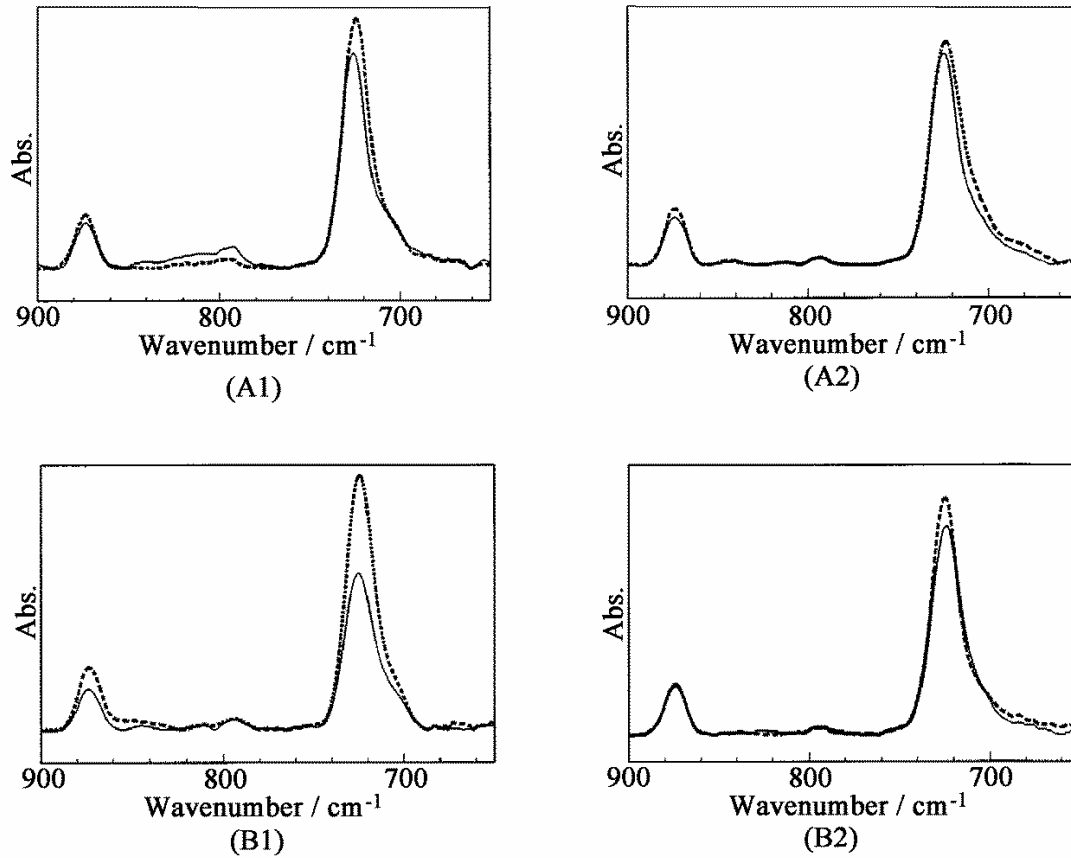


Figure 7. Polarized ATR-IR spectra of PBT₄₀ (A) and PBT₈₀ (B) at the gate. (A1) and (B1) show the spectra for the skin layer and (A2) and (B2) show the spectra for the core layer. The solid and dotted lines correspond to the parallel and perpendicular components, respectively.

comparable. The infrared dichroic ratio at 874 cm^{-1} is plotted in Figure 8. For the skin layer of PBT₄₀, the dichroic ratio was around 0.8, while that of the core layer was about 1.0. Since the dichroic ratio of the skin layer is smaller than that of the core layer, the chain orientation in the skin layer is larger. For PBT₈₀, the dichroic ratio was 0.5 and 0.75 for the skin and core layers, respectively. This also shows higher chain orientation in the skin layer. In addition, the chain orientation for PBT₈₀ was higher than for PBT₄₀ because of larger shear stress at the fast molding rate. The dichroic ratio was almost constant, below around 200 μm , at the surface for both PBTs. This indicates that the boundary between the skin and core layers was comparable with the previous result [1]. The PBT at the surface received a larger share of stress from the mold wall such that the molecular chain oriented along the direction from

the gate to the end, and more mesophase was formed. However, the core layer has a smaller share of stress from the mold plate, and hence less mesophase was formed.

Chain orientation at the end part of the mold plate

At the gate part of the mold plate, the injection molding rate is closely related to the chain orientation. However, at the end part, the molecular chains encounter a wall, causing them to change direction, and hence the chain orientation at the end part was investigated by polarized ATR-IR. Figure 9 shows polarized ATR-IR spectra for PBT₄₀ and PBT₈₀. For the skin layer, the peak intensities of the parallel and perpendicular components are comparable for both PBT₄₀ and PBT₈₀, indicating reduced orientation. However, the intensity ratios between the parallel and

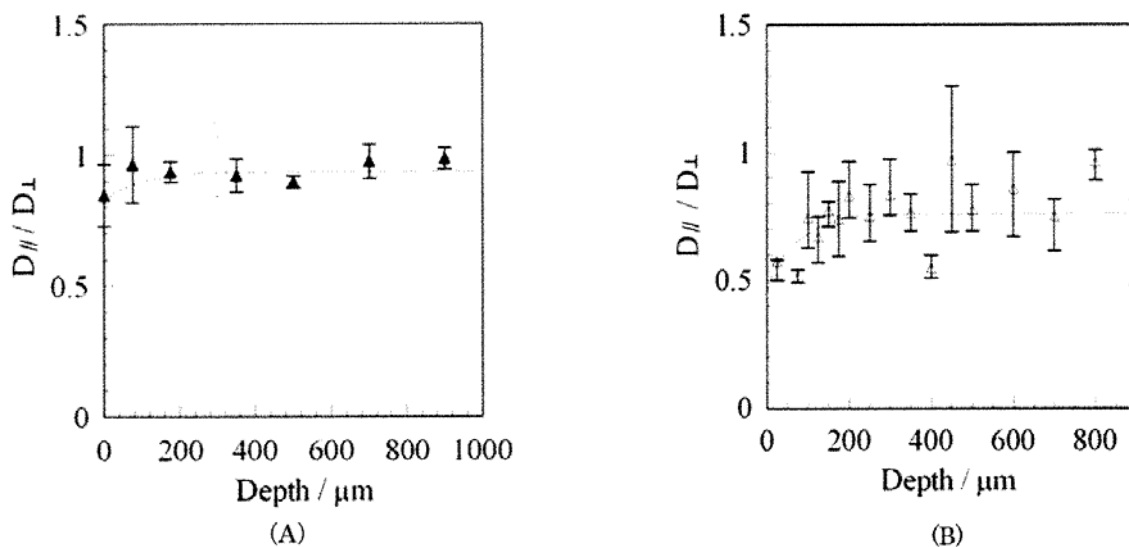


Figure 8. Dichroic ratio of the gate part for PBT₄₀ (A) and PBT₈₀ (B) at 874 cm⁻¹.

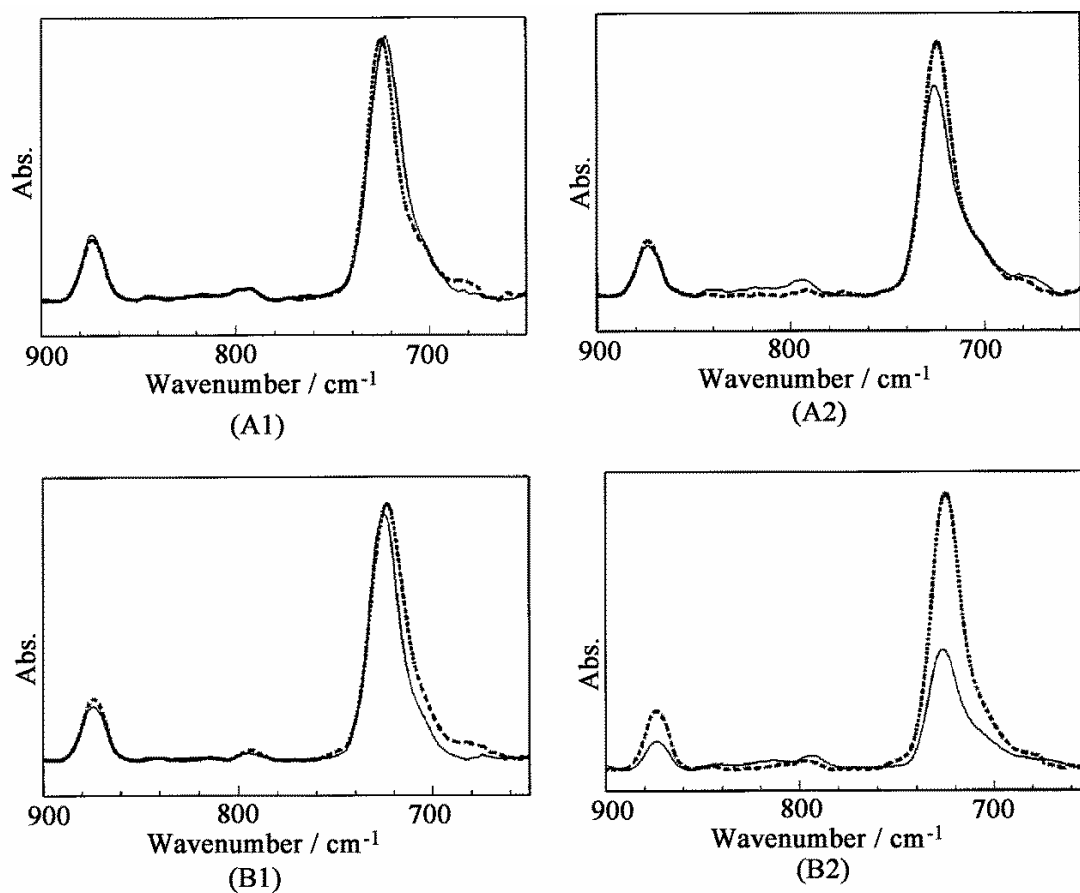


Figure 9. Polarized ATR-IR spectra of PBT₄₀ (A) and PBT₈₀ (B) at the end. (A1) and (B1) show the spectra for the skin layer and (A2) and (B2) show the spectra for the core layer. The solid and dotted lines correspond to the parallel and perpendicular components, respectively.

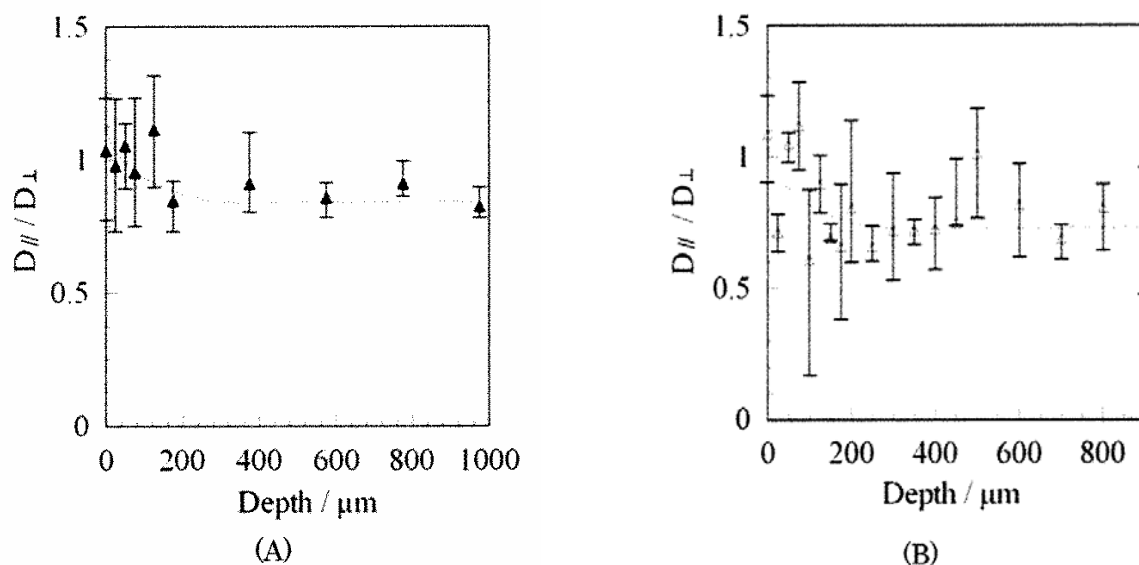


Figure 10. Dichroic ratio of the end part for PBT₄₀ (A) and PBT₈₀ (B) at 874 cm⁻¹.

perpendicular components are larger for the core layer. Figure 10 shows a plot of the dichroic ratio at 874 cm⁻¹. The dichroic ratio was about 1.0 for the skin layer and gradually decreased to 0.8 and 0.7 for the core layer for PBT₄₀ and PBT₈₀, respectively. These results show that there is less chain orientation in the skin layer than in the core layer. This showed the opposite trend to the gate part. The experimental result is difficult to explain, but the chain flux was disturbed at the end of the mold plate and changed direction at the skin layer because the chain flux was fast, resulting in less chain orientation. However, the chain flux in the core layer is comparatively slow such that the chain orientation was retained. However, the interpretation of this result requires further investigation, such as molecular simulation.

CONCLUSIONS

The crystallinity was estimated by DSC for sliced injection-molded PBT formed at injection molding rates of 40 and 80 mm/s. The crystallinity was highest in the skin layer but small in the core layer. However, this result and the result obtained by X-ray diffraction are not in agreement; i.e., according to the results obtained by X-ray diffraction, a lower crystallinity in the skin layer was observed than that in the core layer. The difference in the crystallinity determined by DSC

and X-ray diffraction can be explained by the formation of a mesophase with a liquid crystal-like structure. The fraction of mesophase in PBT₈₀ was larger than that in PBT₄₀ owing to the large shear stress in PBT₈₀. To determine the relationship between the formation of mesophase and the shear, polarized ATR-IR was performed at different depth profiles. At the gate of the mold plate, the infrared dichroic ratio at 874 cm⁻¹ near the skin layer was larger than that at the core layer. This indicates that the chain orientation is higher in the skin layer because of shear stress. On the contrary, at the end part of the mold plate, the dichroic ratio at 874 cm⁻¹ was larger for the core layer. This is because the streaming chains encounter the mold wall and change direction.

ACKNOWLEDGEMENT

We are gratefully thankful to Toyobo Co., Ltd. for the financial support. We also thank Dr. Tomari at Osaka Research Institute of Industrial Science and Technology for allowing us to use the microtome.

CONFLICT OF INTEREST STATEMENT

There are no conflicts of interest.

REFERENCES

1. Hobbs, S. Y. and Pratt, C. F. 1975, *J. App. Polym. Sci.*, 19, 1701.

2. Engberg, K., Ekblad, M., Werner, P. E. and Gedde, U. W. 1994, *Polym. Eng. Sci.*, 34, 1346.
3. Callear, J. E. and Shortall, J. B. 1977, *J. Mater. Sci.*, 12, 141.
4. Katti, S. S. and Schultz, J. M. 1982, *Polym. Eng. Sci.*, 22, 1001.
5. Russell, D. P. and Beaumont, P. W. R. 1980, *J. Mater. Sci.*, 15, 197.
6. Hine, P. J. and Duckett, A. 2004, *Polym. Comp.*, 25, 237.
7. Rhoades, A. M., Williams, J. L., Wonderling, N., Androsch, R. and Guo, J. 2017, *J. Therm. Anal. Calorim.*, 127, 939.
8. Shibaya, M., Ishihara, H., Yamashita, K., Yoshihara, N. and Nonomura, T. 2003, *Seikei-Kakou*, 15, 823.
9. Shibaya, M., Ishihara, H., Yamashita, K., Yoshihara, N. and Nonomura, C. 2004, *International Polymer Processing*, 19, 303.
10. Mencik, Z. J. 1975, *Polym. Sci. Polym. Phys. Ed.*, 13, 2173.
11. Jakeways, R., Ward, I. M., Wilding, M. A., Hall, I. H., Desborough, I. J. and Pass, M. G. 1975, *J. Polym. Sci. Polym. Phys. Ed.*, 13, 799.
12. Joly, A. H., Nemoz, G., Douillard, A. and Vallet, G. 1975, *Makromol. Chem.*, 176, 479.
13. Yokouchi, M., Sakakibara, Y., Chatani, Y., Tadokoro, H., Tanaka, T. and Yoda, K. 1976, *Macromolecules*, 9, 266.
14. Hall, I. H. and Pass, M. G. 1976, *Polymer*, 17, 807.
15. Desborough, I. J. and Hall, I. H. 1977, *Polymer*, 18, 825.
16. Nitzsche, S. A., Wang, Y. K. and Hsu, S. L. 1992, *Macromolecules*, 25, 2397.
17. Apostolov, A. A., Fakirov, S., Stamm, M., Patil, R. D. and Mark, J. E. 2000, *Macromolecules*, 33, 6856.
18. García-Gutiérrez, M. C., Hernández, J. J., Nogales, A., Panine, P., Rueda, D. R. and Ezquerra, T. A. 2008, *Macromolecules*, 41, 844.
19. Takahashi, Y., Murakami, K. and Nishikawa, S. 2002, *J. Polym. Sci. Part B: Polym. Phys.*, 40, 765.
20. Righetti, M. C., Di Lorenzo, M. L., Angiuli, M. and Tombari, E. 2004, *Macromolecules*, 37, 9027.
21. Konishi, T. and Miyamoto, Y. 2010, *Macromolecules*, 43, 375.
22. Song, K. 2000, *J. Appl. Polym. Sci.*, 78, 412.
23. Li, L. and de Jeu, W. H. 2004, *Macromolecules*, 37, 5646.
24. Mago, G., Fisher, F. T. and Kalyon, D. M. 2008, *Macromolecules*, 41, 8103.
25. Pyda, M., Nowak-Pyda, E., Mays, J. and Wunderlich, B. 2004, *J. Polym. Sci. Polym. Phys.*, 42, 4401.